

## Reducing background effects in orchards through spectral vegetation index correction



Jonathan Van Beek<sup>a,\*</sup>, Laurent Tits<sup>a</sup>, Ben Somers<sup>b</sup>, Tom Deckers<sup>c</sup>, Pieter Janssens<sup>d</sup>, Pol Coppin<sup>a</sup>

<sup>a</sup> KU Leuven, Department of Biosystems, M3-BIORES, Willem de Croylaan 34, Leuven BE-3001, Belgium

<sup>b</sup> KU Leuven, Division Forest, Nature and Landscape, Celestijnenlaan 200E, Leuven BE-3001, Belgium

<sup>c</sup> Pcfuit Research Station, Fruittuinweg 1, Sint-Truiden BE-3800, Belgium

<sup>d</sup> Soil Service of Belgium, Willem de Croylaan 48, Leuven BE-3001, Belgium

### ARTICLE INFO

#### Article history:

Received 4 March 2014

Accepted 15 August 2014

#### Keywords:

Biophysical variables

Mixture problem

Orchards

Canopy cover fraction

Vegetation indices

Signal unmixing

### ABSTRACT

Satellite remote sensing provides an alternative to time-consuming and labor intensive in situ measurements of biophysical variables in agricultural crops required for precision agriculture applications. In orchards, however, the spatial resolution causes mixtures of canopies and background (i.e. soil, grass and shadow), hampering the estimation of these biophysical variables. Furthermore, variable background mixtures obstruct meaningful comparisons between different orchard blocks, rows or within each row. Current correction methodologies use spectral differences between canopies and background, but struggle with a vegetated orchard floor. This background influence and the lack of a generic solution are addressed in this study.

Firstly, the problem was demonstrated in a controlled environment for vegetation indices sensitive to chlorophyll content, water content and leaf area index. Afterwards, traditional background correction methods (i.e. soil-adjusted vegetation indices and signal unmixing) were compared to the proposed vegetation index correction. This correction was based on the mixing degree of each pixel (i.e. tree cover fraction) to rescale the vegetation indices accordingly and was applied to synthetic and WorldView-2 satellite imagery. Through the correction, the effect of background admixture for vegetation indices was reduced, and the estimation of biophysical variables was improved ( $\Delta R^2 = 0.2-0.31$ ).

© 2014 Elsevier B.V. All rights reserved.

## 1. Introduction

Precision agriculture in orchards requires accurate, reliable and continuous information at high spatial and temporal scales (Pinter et al., 2003), sensitive to stress-related biophysical variables such as chlorophyll content (Zarco-Tejada et al., 2004), water content (Govender et al., 2009) and leaf area index (LAI). In situ measurements of these biophysical variables are time-consuming and labor intensive, while technological advances in remote sensing provide non-destructive, time efficient and cost beneficial alternatives (Dorigo et al., 2007). For precision farming in deciduous orchard

growing regions, the high cloud cover requires a near-to-daily revisit time to provide consistent information throughout the growing season (Moran et al., 2003). Furthermore, the high spatial variability in orchards (Perry et al., 2009) requires high spatial resolution imagery to provide accurate information essential for steering precision farming management schemes. Currently, this combination of both high spatial and temporal resolution data is feasible from high spatial resolution satellite sensors with off-nadir viewing capabilities, such as GeoEye-1, Quickbird, Pleiades or WorldView-1 and WorldView-2.

Despite the relatively high spatial resolution of these satellite sensors, remote sensing imagery over orchards will contain mixtures of canopies and backgrounds (i.e. soil, grass and shadow). Even at sub-meter spatial resolution, this mixture of canopies and background will be present (Stuckens et al., 2010). Furthermore, the combination of satellite imagery with a high spatial resolution (i.e. 2 m) and orchard geometry (i.e. row planting distance) will also cause variable background mixtures, obstructing meaningful

\* Corresponding author. Tel.: +32 1632 8146; fax: +32 1632 2966.

E-mail addresses: [jonathan.vanbeek@biw.kuleuven.be](mailto:jonathan.vanbeek@biw.kuleuven.be) (J. Van Beek), [laurent.tits@biw.kuleuven.be](mailto:laurent.tits@biw.kuleuven.be) (L. Tits), [ben.somers@ees.kuleuven.be](mailto:ben.somers@ees.kuleuven.be) (B. Somers), [tom.deckers@pcfuit.be](mailto:tom.deckers@pcfuit.be) (T. Deckers), [pjanssens@bdb.be](mailto:pjanssens@bdb.be) (P. Janssens), [pol.coppin@biw.kuleuven.be](mailto:pol.coppin@biw.kuleuven.be) (P. Coppin).

comparisons between different orchard blocks, rows or within each row. Moreover, the background will be influenced by geological differences, slopes, presence or absence of vegetation and weed species distribution, causing a high spatial variability within one orchard.

In the past, several methods were constructed to remove the influence of the background components. An established way to diminish soil background effects is the use of soil-adjusted vegetation indices combined with TCARI (Transformed Chlorophyll Absorption in Reflectance Index) (Haboudane et al., 2002; Zarco-Tejada et al., 2004). Another technique to minimize or remove background effects in orchards is signal unmixing models (Somers et al., 2009; Tits et al., 2013b), which often require large databases of background spectra to correct imagery and account for spatial variability. However, both these approaches were based on the spectral differences between soil and vegetation, rendering them less usable in orchards with vegetative orchard floors or backgrounds.

Mixture effect could also be avoided by the application of a spatial filtering or smoothing of reflectance or vegetation index values, e.g. Acevedo-Opazo et al. (2008). This approach requires a uniform background and a similar row and tree spacing in order to present similar canopy and background mixtures throughout the orchard. However, both spectral information and spatial variability might be lost due to the smoothing algorithm and comparisons between orchards with different row or tree spacing would cause inaccuracies.

All of the above-described methodologies were able to remove background effects in certain circumstances but did not provide a standard solution for the mixture problem. This lack of a generic solution to reduce background effects irrespective of background types (i.e. soil, grass and shadow) and the influence of variable background mixtures on vegetation indices require further investigation. Therefore, this study addresses the mixture problem in orchards presented in high spatial resolution space borne imagery. Through synthetic imagery, the mixture problem was demonstrated in a controlled environment for different background scenarios toward the estimation of biophysical variables (i.e. chlorophyll, water content and LAI). A vegetation index correction method, based on the canopy cover fractions, was tested in the virtual environment and afterwards implemented on space borne imagery of a commercial hedgerow pear orchard.

## 2. Materials

### 2.1. Synthetic images

Synthetic or simulated imagery provide a useful data source for improving our understanding of remotely sensed data and are frequently used to perform a preliminary evaluation of analysis techniques, e.g. Tits et al. (2013b). The advantages of synthetic data are the availability of the exact cover fractions, spectral signatures and the biophysical variables of the target crop. In this study, the simulations were used to demonstrate the mixed pixel problem in orchard crops, to visualize its effect on vegetation indices, to prove the necessity of a correction method and to quantify the improvements of the proposed correction algorithm.

A virtual orchard, developed by Stuckens et al. (2009), was modified and adapted for this study. The virtual orchard consisted of virtual citrus trees (*Citrus sinensis* L.), comprises triangular meshes (Weber and Penn, 1995), for which the leaf and stem optical properties and physical properties were based on field measurements (Somers et al., 2009; Stuckens et al., 2009). The virtual trees were arranged in a 3.5 m × 2 m grid with a row azimuth of 7°.

In the virtual orchard, three biophysical variables were investigated, i.e. chlorophyll, water and LAI. For each variable, several

**Table 1**

The mean, standard deviation ( $\sigma$ ) and range of chlorophyll, water content and leaf area index for the unmodified trees used in the virtual orchard.

Biophysical variable	Mean value ( $\pm\sigma$ )	Range
Chlorophyll content ( $\mu\text{g}/\text{cm}^2$ )	38.69 ( $\pm 10.55$ )	16.08–58.92
Water content ( $\text{mg}/\text{cm}^2$ )	18.81 ( $\pm 2.35$ )	13.43–21.63
Leaf area index ( $\text{cm}^2/\text{cm}^2$ )	6.44 ( $\pm 1.72$ )	3.20–10.97

sections of the virtual orchard were modified to mimic stressed conditions. The leaf optical properties of these virtual trees were modified by extracting the biophysical variables from the unmodified spectra through the inversion of PROSPECT (Jacquemoud and Baret, 1990), and lowering the extracted variables to 50% and 75% of the original value for chlorophyll and to 70% and 85% of the original value for water content. Afterwards, the modified spectra were recalculated through PROSPECT with the modified variables (Stuckens et al., 2009). For LAI, the virtual trees were modified by randomly removing or adding leaves to represent 125% and 56% of the original LAI (Stuckens et al., 2009). An overview of the used biophysical variables is shown in Table 1, while the spatial distribution of each biophysical variable is represented in Fig. 1a, b and d.

From these virtual orchards, different images were made in a physically based ray-tracer (PBRT, Pharr and Humphreys, 2004), with a direct and diffuse illumination source (elevation of 79.2° and azimuth of 339.6°), corresponding to the position of the sun on Southern summer solstice on 22nd of December in 2007 at 13:00 h. The sensor was positioned in zenith, and combined with an orthographic projection to yield images without any geometric distortion. The spectral range of the synthetic image was 350–2500 nm with a spectral resolution of 10 nm, while the spatial resolution of the sensor was fixed at 2 m. The resulting canopy cover fractions within the 2 m pixels are shown in Fig. 1e.

The influence of different background types was investigated by varying the orchard floor or background through three different scenarios, while the position of the virtual trees remained identical for each scenario.

- Scenario 1 (S1), a uniform soil background, consisting of an Albic Leptic Luvisol soil (FAO, 1988), for which the reflectance was measured in situ (Somers et al., 2010). An RGB image of the orchard with the uniform soil background is shown in Fig. 1c.
- Scenario 2 (S2), a uniform weed background, consisting of *Phleum pratense* L. modeled with leaf reflectance obtained from the Leaf Optical Experiment database (Hosgood et al., 1994; Stuckens et al., 2009).
- Scenario 3 (S3), a variable weed background, consisting of a weed background with a chlorophyll gradient. The weed background was modified similar to the leaf reflectances, increasing the chlorophyll content from 75% to the reference value (i.e. uniform weed background). The spatial distribution of the variable weed background is depicted in Fig. 1f.

S1 was used to investigate the usefulness of existing background correction methodologies (i.e. soil-adjusted vegetation indices and signal unmixing), while S2 was used to link this to variable conditions (S3).

### 2.2. Study area and satellite imagery

Satellite imagery was acquired over an orchard, planted with Conference pear trees (*Pyrus communis* L. cv. 'Conference'), situated in Bierbeek, Belgium (50°49'34.59" N 4°47'42.83" E). The  $\pm 2.5$  m high trees were planted between 1989 and 2010 in a 3.5 m × 1 m grid (row azimuth 41°) and trained into either a V-system with

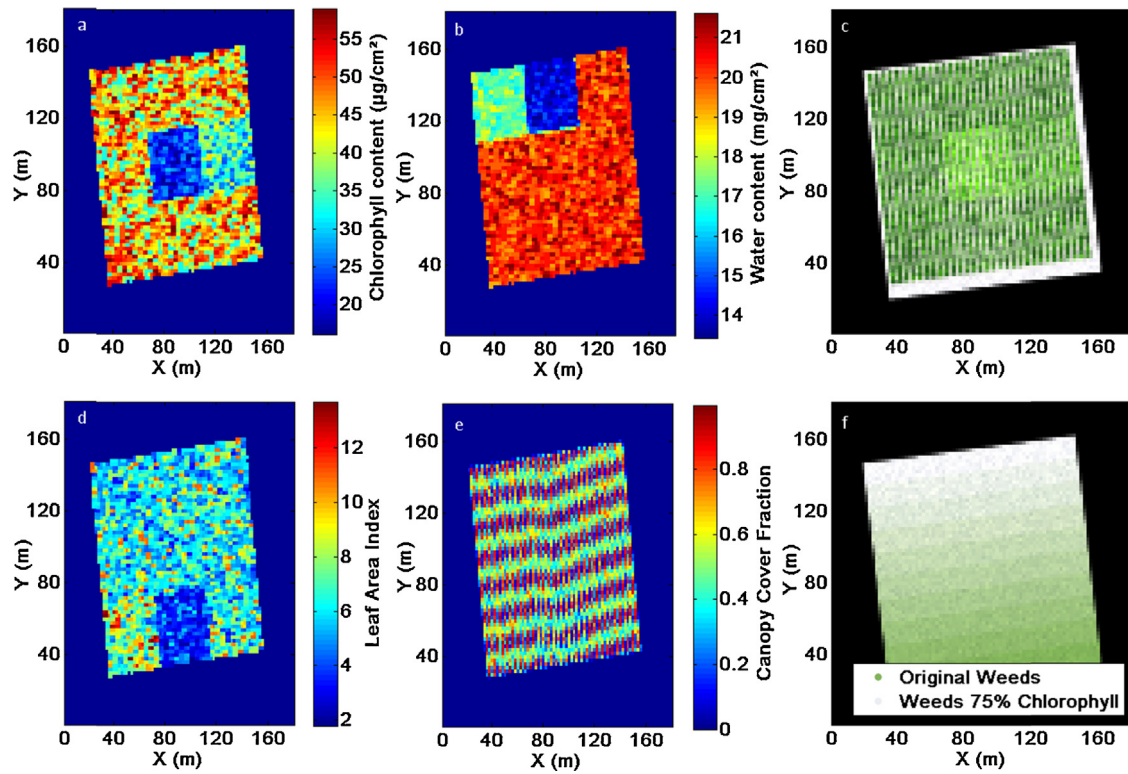


**Fig. 1.** Spatial distribution of biophysical variables in the virtual orchard for chlorophyll content (a), water content (b) and leaf area index (d), together with an RGB image of the orchard (c), the canopy cover fractions (e) and the spatial distribution of chlorophyll content of the background for Scenario 3, the variable weed background (f). For a color representation of the figures, the reader is referred to the web version of this article.

four fruiting branches on one central stem or a spindle bush system (Sansavini and Musacchi, 1994). Grass was sown in between the tree rows.

The WorldView-2 satellite sensor was used in this study because of the possibilities toward agriculture through the inclusion of a red-edge band (705–745 nm) (Marchisio et al., 2010) and a high revisit time, insuring the presence of imagery at requested times. Other sensors with similar spatial resolutions would present a similar variable background mixture. In addition, WorldView-2 satellite imagery was used in this study because it was previously used to study water status of pear trees (Van Beek et al., 2013). A WorldView-2 multispectral image was acquired in 2012 on DOY 148, with a 2 m spatial resolution, a 2.7° off-nadir viewing angle and a satellite azimuth and elevation angle of 181.1° and 86.7°, respectively. Based on metadata provided by the manufacturer (DigitalGlobe), radiometric correction was carried out through the application of gain and offset (Uptike and Comp, 2010). Afterwards, atmospheric influences were removed through Fast Line-of-sight Atmospheric Analysis of Spectral Hypercubes (Adler-Golden et al., 1998).

### 3. Methods

#### 3.1. Vegetation indices

In this study, vegetation indices were used to estimate the biophysical variables from the synthetic images. The GM1 index (Gitelson and Merzlyak, 1996) was related to chlorophyll content, the Normalized Difference SWIR Index (NDSI; this study) to water content and the standardized LAI Determining Index (sLAI DI; Delalieux et al., 2008) to LAI. The strength of correlation between biophysical variables and vegetation indices was determined with

the coefficient of determination ( $R^2$ ) and the Root Mean Squared Error (RMSE).

$$GM1 = \frac{R_{750}}{R_{550}} \quad (1)$$

$$NDSI = \frac{R_{1750} - R_{1800}}{R_{1750} + R_{1800}} \quad (2)$$

$$sLAI DI = S \times \left[ \frac{R_{1050} - R_{1250}}{R_{1050} + R_{1250}} \right] \quad (3)$$

$$R^2 = 1 - \sum \frac{(y - y_{pred})^2}{S(y - y_{mean})^2} \quad (4)$$

$$RMSE = \sqrt{\sum (y_{pred} - y)^2} \quad (5)$$

where  $R_x$  is the reflectance at wavelength  $x$ ;  $S$  a scaling factor equal to 5;  $y$  the measured biophysical variable;  $y_{pred}$  the predicted biophysical variable and  $y_{mean}$  the average biophysical variable.

For the multispectral satellite imagery (Section 2.2), the Red-Edge Normalized Difference Vegetation Index (ReNDVI; Van Beek et al., 2013) was applied, a normalized difference ratio between the NIR 1 (Near-Infrared; 770–895 nm) and Red-edge (705–745 nm) bands of WorldView-2. ReNDVI was previously linked to water status in irrigated and non-irrigated pear orchards (Van Beek et al., 2013) and should represent a low spatial variability as all trees received similar irrigation amounts.

$$ReNDVI = \frac{R_{NIR1} - R_{Red-Edge}}{R_{NIR1} + R_{Red-Edge}} \quad (6)$$

#### 3.2. Canopy fraction estimation

For the synthetic images, the exact tree cover was known for each pixel. For the real satellite imagery, the canopy cover fraction

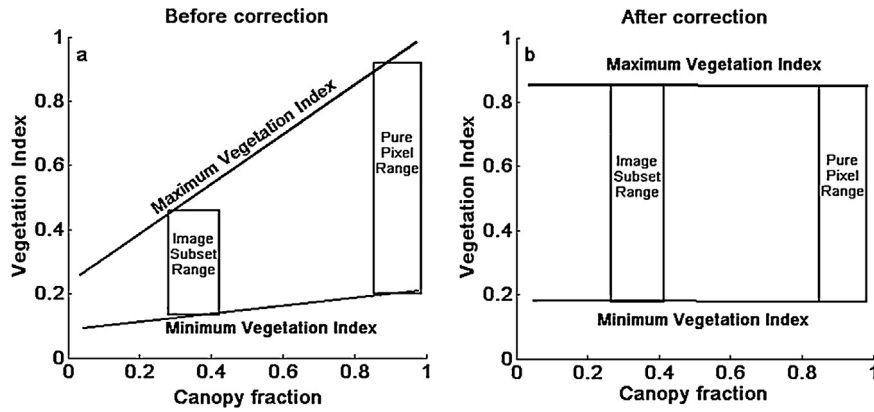


Fig. 2. Schematic representation of the relation between canopy fraction and vegetation index, before (a) and after correction (b).

was estimated through a Gram-Schmidt pan-sharpening (Laben and Brower, 2000) to produce multispectral bands with a panchromatic resolution (0.5 m). This pan-sharpened image was classified through unsupervised classification (Tou and Gonzalez, 1974) and resampled for each 2 m multispectral pixel to provide an estimation of the canopy fractions, similar to Hamada et al. (2011).

### 3.3. Traditional background correction

#### 3.3.1. Soil-adjusted vegetation indices

A traditional method to bypass the background effects on images was the use of soil-adjusted vegetation indices (Huete, 1988; Rondeaux et al., 1996). In this study, both TCARI/OSAVI (Transformed Chlorophyll Absorption in Reflectance Index/Optimization of Soil-Adjusted Vegetation Indices) and MCARI/OSAVI (Modified Chlorophyll Absorption in Reflectance Index/Optimization of Soil-Adjusted Vegetation Indices) ratios were applied to S1, as they were previously shown to mitigate the effects of a soil background, while being relatively insensitive to canopy cover variations (Haboudane et al., 2002; Zarco-Tejada et al., 2004).

$$OSAVI = (1 + 0.16) \times \frac{R_{800} - R_{670}}{R_{800} - R_{670} + 0.16} \quad (7)$$

$$TCARI = 3 \times (R_{700} - R_{670}) - 0.2 \times (R_{700} - R_{550}) \times \left( \frac{R_{700}}{R_{670}} \right) \quad (8)$$

$$MCARI = [(R_{700} - R_{670}) - 0.2 \times (R_{700} - R_{550})] \times \left( \frac{R_{700}}{R_{670}} \right) \quad (9)$$

#### 3.3.2. Signal unmixing

Next to soil-adjusted vegetation indices, signal unmixing was applied to remove or reduce background effects. Alternating Least Squares (ALS) was chosen as it was an established Chemometrics methodology to estimate both the absorption spectrum and concentration of different components (Tauler et al., 1993). Recently, it was successfully applied to the unmixing problem in remote sensing (Tits et al., 2013a), to avoid the requirement of large databases for traditional signal unmixing models, such as MESMA (Roberts et al., 1998). In ALS, each set of four adjacent pixels was used to iteratively estimate canopy spectral signatures for the four mixed pixels. For this, the ALS model required a starting estimate of both the background and canopy spectra. In this instance, the pure tree spectra were averaged for the entire orchard, together with an average soil background, similar to (Tits et al., 2013a), based on field measurements (Somers et al., 2009).

### 3.4. Vegetation index correction

In the proposed vegetation index correction method, the range of index values for all pixels was rescaled to the range of index values for the pure canopy pixels (i.e. pixels with a canopy fractions over 0.8), assuming that the range of index values for the pure canopy pixels was non-contaminated and representative for the true range of index values (or biophysical variables). A graphical representation is shown in Fig. 2 and comprised the following steps:

- For each mixed pixel, the distribution of index values from pixels with similar canopy fractions (i.e. within a canopy fraction range of 0.05) was determined (left box in Fig. 2a).
- All index values in the selected box were rescaled to the index value range present in the pure canopy pixels (right box in Fig. 2a).
- As a subset was defined and rescaled for every pixel individually for all possible canopy fraction subsets (within a range of 0.05), each image pixel will be rescaled multiple times. Only the average index value was retained in the further analysis (left box in Fig. 2b).

Overall, this correction assumed that the variability along the y-axis (i.e. vegetation index value) was only caused by the variability in tree conditions, while the variability along the x-axis (i.e. canopy fraction) was caused by the admixture of the background component. This is true if no variability in the background is present (e.g. uniform soil scenario) or if the variable background does not influence the vegetation index value. As both cases only seldom occur, a moving window approach needs to be applied for scenarios with a variable background (e.g. variable weed background scenario and real conditions). Within each moving window, some assumptions were made, namely (i) the uniformity of the background, (ii) the representation of the true vegetation index range in the pure canopy pixels for that moving window and (iii) the presence of the full range of canopy fractions. To fulfill these criteria, a moving window size of  $7 \times 7$  pixels was found to represent all canopy fractions. Within each moving window, the range of vegetation indices was rescaled to the range of the pure canopy pixels within that moving window. Afterwards, the index values for each pixel were averaged from all the moving windows which included that pixel.

Before the correction was applied, outliers were detected and removed, based on the threshold of 1.5 times the inter-quartile range from the upper or lower quartile (Laurikkala et al., 2000).

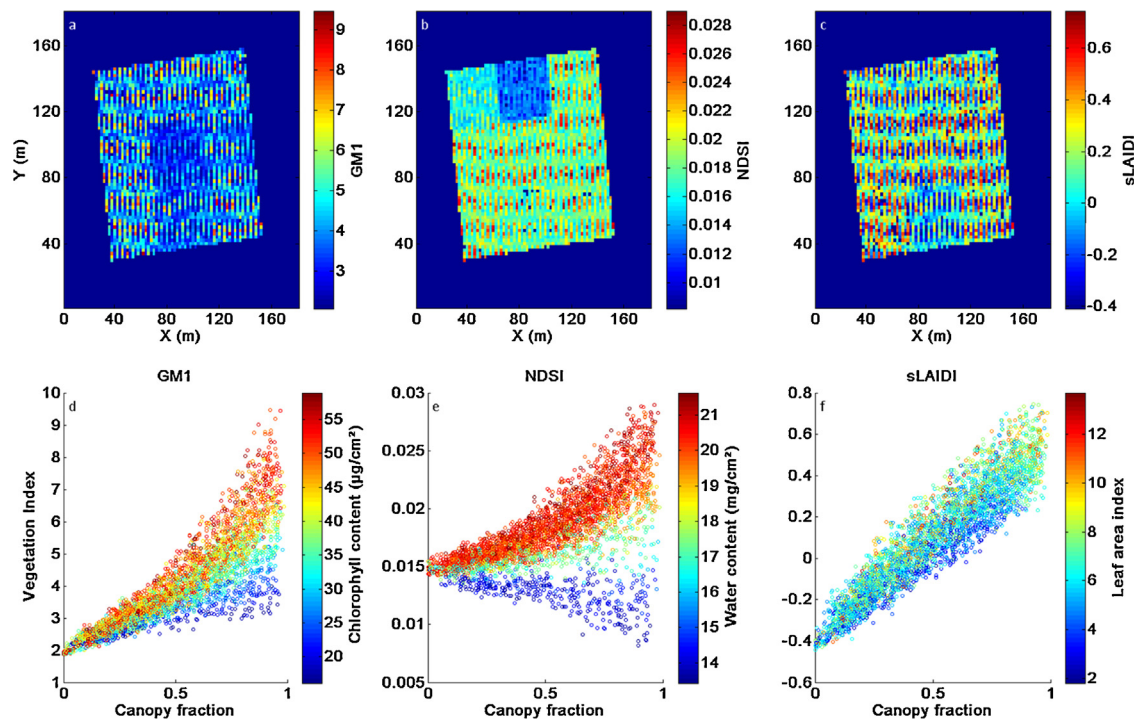


**Fig. 3.** Uniform soil background synthetic images and scatter plots before correction of the GM1 index (a and d), the NDSI (b and e) and the sLAIDI (c and f). All points were labeled for chlorophyll content ( $\mu\text{g}/\text{cm}^2$ ), water content ( $\text{mg}/\text{cm}^2$ ) and leaf area index.

## 4. Results

### 4.1. Synthetic images: uniform soil background (S1)

In the synthetic images, the influence of the mixture could be investigated because the exact cover fraction of all components was known. The relation between canopy fractions and vegetation indices (Section 3.1) for the uniform soil background scenario is shown in Fig. 3.

The expected spatial distribution of the biophysical variables (Fig. 1a, b and d) was not visible in the vegetation index images (Fig. 3a–c) and although the modified regions were highlighted, mixed pixels would also be classified as modified/stressed. The resulting striped pattern was the result of an alternation between pure and mixed canopy cover fractions, also visible in Fig. 1e. These dependencies of the index values on canopy cover fractions were also shown in the scatterplots (Fig. 3d–f). As such, these results demonstrated the necessity of a correction (Section 3.4).

#### 4.1.1. Vegetation index correction

The results of the correction are depicted in Fig. 4. Through the correction, the canopy fraction dependency of the vegetation indices was removed. The modified regions within the orchard were clearly visible (Fig. 4a–c), while the differences within each management block were minimized.

The improvement of the correction method was indicated by the  $R^2$  and RMSE values between vegetation indices and biophysical variables before and after correction, shown in Table 2. The correlation between chlorophyll content and the GM1 index improved ( $\Delta R^2 = 0.31$ ;  $\Delta \text{RMSE} = -1.76 \mu\text{g}/\text{cm}^2$ ). A similar improvement was observed between water content and NDSI ( $\Delta R^2 = 0.35$ ;  $\Delta \text{RMSE} = -0.5 \text{mg}/\text{cm}^2$ ). On the other hand, the insignificant relation between LAI and sLAIDI before and after correction ( $\Delta R^2 = 0.07$ ;  $\Delta \text{RMSE} = 0.07 \text{cm}^2/\text{cm}^2$ ), was most likely caused by interference of water content, for which the stressed region was represented in the corrected index image (Fig. 4f).

For lower canopy cover fractions some discrepancies remained, as small differences related to canopy-background interactions and shadow were enlarged. A canopy cover threshold was applied, as pixels with small canopy cover fractions are less important to end-users and introduce large errors related to small differences. All pixels with canopy cover fractions above 0.4 were retained, similar to Somers et al. (2009), to quantify the usable improvement of the correction. With the exception of LAI, the  $R^2$  values between biophysical variables and index values increased significantly after the application of the canopy cover threshold compared to the uncorrected results ( $\Delta R^2 = 0.39$  and  $0.41$ ; Table 2).

#### 4.1.2. Traditional background correction

The relationship between both the TCARI/OSAVI and MCARI/OSAVI ratios and the canopy cover fractions are depicted in Fig. 5. Although both TCARI/OSAVI ( $R^2 = 0.27$ ;  $\text{RMSE} = 7.92 \mu\text{g}/\text{cm}^2$ ) and MCARI/OSAVI ( $R^2 = 0.11$ ;  $\text{RMSE} = 8.8 \mu\text{g}/\text{cm}^2$ ) showed a better relation with chlorophyll content before correction ( $R^2 = 0.09$ ;  $\text{RMSE} = 9.39 \mu\text{g}/\text{cm}^2$ ), the results still showed some dependencies toward canopy fraction and less correlation compared to the vegetation index correction results ( $R^2 = 0.40$ ;  $\text{RMSE} = 7.63 \mu\text{g}/\text{cm}^2$ ).

Through the ALS algorithm (Section 3.3.2; Table 2), improvements similar to the vegetation index correction were observed between vegetation indices and biophysical variables ( $R^2 = 0.39$ ;  $\text{RMSE} = 7.71 \mu\text{g}/\text{cm}^2$  for chlorophyll content and  $R^2 = 0.63$ ;  $\text{RMSE} = 1.26 \text{mg}/\text{cm}^2$  for water content). These results showed that ALS was able to remove background effects in orchards with soil backgrounds.

## 4.2. Synthetic images: weed background

### 4.2.1. Uniform weed background (S2)

For S2 the index values showed a similar dependency to the canopy cover fraction. Because of the similarities with Figs. 3 and 4, the index images and scatter plots are not

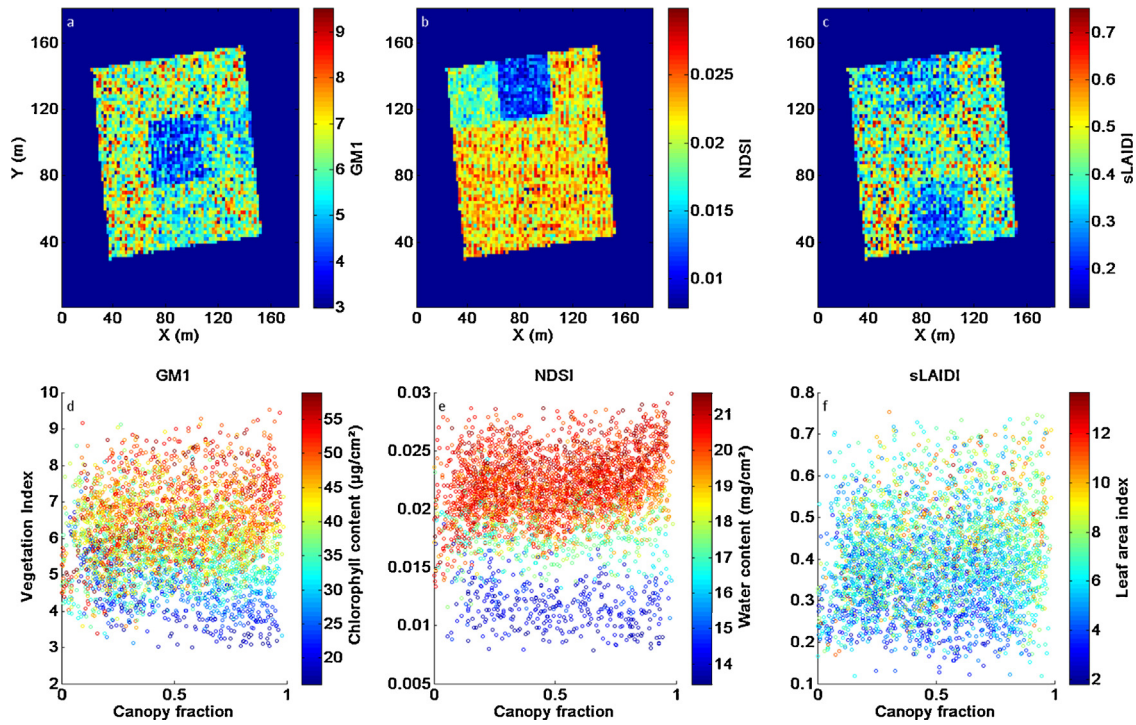


Fig. 4. Uniform soil background synthetic images and scatter plots after correction of the GM1 index (a and d), the NDSI (b and e) and the sLAIDI (c and f). All points were labeled for chlorophyll content ( $\mu\text{g}/\text{cm}^2$ ), water content ( $\text{mg}/\text{cm}^2$ ) and leaf area index.

shown. Through the correction method, most of the background effects were removed for chlorophyll content ( $R^2 = 0.51\text{--}0.56$ ;  $\text{RMSE} = 6.88\text{--}6.50 \mu\text{g}/\text{cm}^2$ ) and water content ( $R^2 = 0.64\text{--}0.74$ ;  $\text{RMSE} = 1.22\text{--}1.04 \text{mg}/\text{cm}^2$ ). The correlation between LAI and sLAIDI was insignificant ( $R^2 = 0.13\text{--}0.14$ ;  $\text{RMSE} = 1.89\text{--}1.82 \text{cm}^2/\text{cm}^2$ ), similar to S1.

For S2, the ALS algorithm (Section 3.3.2; Table 2) decreased the correlation between GM1 and chlorophyll content ( $R^2 = 0.42$ ;  $\text{RMSE} = 7.43 \mu\text{g}/\text{cm}^2$ ), indicating that ALS was unable to remove background effects in orchards with weed backgrounds as a result of the spectral similarity between canopies and background.

4.2.2. Variable weed background (S3)

One of the assumptions made in the previous section was the uniformity of the background, so that vegetation index variations were only caused by the variability in tree conditions for similar canopy fractions. For variable background scenarios, such as S3, the vegetation index variations were not solely caused by canopy conditions, indicated by the variability for pixels with a high background contribution (Fig. 6d). Therefore, a moving window approach was applied to correct S3 (Section 3.4). The synthetic images before and after correction, together with the scatter plot for each biophysical variable are shown in Figs. 6 and 7, respectively.

**Table 2**  
Coefficient of determination ( $R^2$ ) and Root Mean Squared Error (RMSE) before and after correction for canopy cover variations (Section 3.4) for the uniform soil background scenario (S1), for the soil-adjusted vegetation indices for the uniform soil background scenario (TCARI/OSAVI and MCARI/OSAVI), the uniform soil background scenario with ALS correction (S1 ALS correction), the uniform weed scenario (S2), the uniform weed background scenario with ALS correction (S2 ALS correction) and the variable weed scenario (S3). The  $R^2$  and RMSE were calculated for all the pixels and for pixels with a canopy cover over 0.4 (Canopy threshold 0.4). In addition, the metrics of the reference canopies are depicted, extracted from virtual orchards with similar light conditions but without background.

Scenario	Biophysical variable	Reference canopies		Before correction		After correction		Canopy threshold 0.4	
		$R^2$	RMSE	$R^2$	RMSE	$R^2$	RMSE	$R^2$	RMSE
S1	Chlorophyll content ( $\mu\text{g}/\text{cm}^2$ )	0.79	5.15	0.09	9.39	0.40	7.63	0.57	6.46
	Water content ( $\text{mg}/\text{cm}^2$ )	0.75	1.14	0.31	1.71	0.66	1.21	0.72	1.10
	Leaf area index ( $\text{cm}^2/\text{cm}^2$ )	0.74	1.23	0.07	1.89	0.14	1.82	0.18	1.77
TCARI/OSAVI MCARI/OSAVI	Chlorophyll content ( $\mu\text{g}/\text{cm}^2$ )	–	–	0.27	7.92	–	–	–	–
	Chlorophyll content ( $\mu\text{g}/\text{cm}^2$ )	–	–	0.11	8.80	–	–	–	–
S1 ALS correction	Chlorophyll content ( $\mu\text{g}/\text{cm}^2$ )	–	–	0.09	9.39	0.39	7.71	–	–
	Water content ( $\text{mg}/\text{cm}^2$ )	–	–	0.31	1.71	0.63	1.26	–	–
	Leaf area index ( $\text{cm}^2/\text{cm}^2$ )	–	–	0.07	1.89	0.13	1.82	–	–
S2	Chlorophyll content ( $\mu\text{g}/\text{cm}^2$ )	0.79	5.15	0.51	6.88	0.56	6.50	0.71	5.38
	Water content ( $\text{mg}/\text{cm}^2$ )	0.75	1.14	0.64	1.22	0.74	1.04	0.80	1.40
	Leaf area index ( $\text{cm}^2/\text{cm}^2$ )	0.74	1.23	0.13	1.80	0.14	1.79	0.18	1.75
S2 ALS correction	Chlorophyll content ( $\mu\text{g}/\text{cm}^2$ )	–	–	0.51	6.88	0.42	7.44	–	–
	Water content ( $\text{mg}/\text{cm}^2$ )	–	–	0.64	1.22	0.70	1.03	–	–
	Leaf area index ( $\text{cm}^2/\text{cm}^2$ )	–	–	0.13	1.80	0.14	1.80	–	–
S3	Chlorophyll content ( $\mu\text{g}/\text{cm}^2$ )	0.79	5.15	0.37	7.93	0.57	6.51	0.64	6.16
	Water content ( $\text{mg}/\text{cm}^2$ )	0.75	1.14	0.63	1.22	0.76	0.77	0.78	0.97
	Leaf area index ( $\text{cm}^2/\text{cm}^2$ )	0.74	1.23	0.14	1.88	0.13	1.87	0.13	1.85

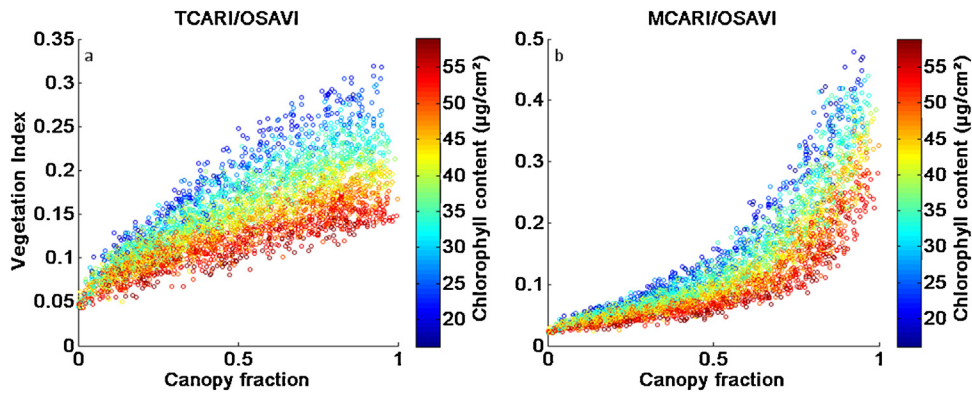


Fig. 5. Canopy fraction against the TCARI/OSAVI ratio index (a) and the MCARI/OSAVI ratio index (b) for S1 with all points labeled for chlorophyll content ( $\mu\text{g}/\text{cm}^2$ ).

Before the correction, the alternation between pure and mixed pixels was visible (Fig. 6a–c), albeit less compared to the uniform soil background (Fig. 3), because of the similarity between canopy and background spectra. On the other hand, the scatter plots of the vegetation indices showed a similar dependency toward canopy fraction (Fig. 6d–f).

After the correction, most of the mixed pixel influences were removed and only the modified regions were contrasted, while the mixed pixels could no longer be confused with stressed/modified canopies. In the corrected vegetation images, some blurred regions were visible (Fig. 7a–b). This was the result of the edge between two stressed/modified regions in combination with mixed pixels (i.e. canopy fraction  $\sim 0.5$ ). For these pixels, 50% of all moving windows included pure canopy pixels of one condition (i.e. stress), while in the other 50% of all moving windows, pure canopy pixels of another condition were included. This caused some very distinct correction results, which after averaging were similar for adjacent pixels. If this would occur, the simple correction method (Section 3.4) would be unable to rectify the background problem.

For chlorophyll and water content, the correlation with GM1 ( $R^2 = 0.37\text{--}0.57$ ;  $\text{RMSE} = 7.93\text{--}6.51 \mu\text{g}/\text{cm}^2$ ) and NDSI ( $R^2 = 0.63\text{--}0.76$ ;  $\text{RMSE} = 1.22\text{--}0.77 \text{mg}/\text{cm}^2$ ), respectively, improved after correction (Table 2), while the relation between LAI and sLAI was insignificant both before and after correction ( $R^2 = 0.14\text{--}0.13$ ;  $\text{RMSE} = 1.88\text{--}1.87 \text{cm}^2/\text{cm}^2$ ).

#### 4.3. Satellite image

From the synthetic imagery, the usefulness and universal use of the correction method was shown. Through a satellite image of a hedgerow orchard, the necessity and usefulness of the vegetation index correction could be further illustrated. In Fig. 8, an RGB image of the orchard in the study area is shown, together with the ReNDVI image before and after correction. The correction was similar to S3, but the pure canopy threshold was lowered to 0.7 because of the low cover fraction presented in the orchard.

The differences between the management blocks in Fig. 8b were mostly related to different management systems (i.e. central block

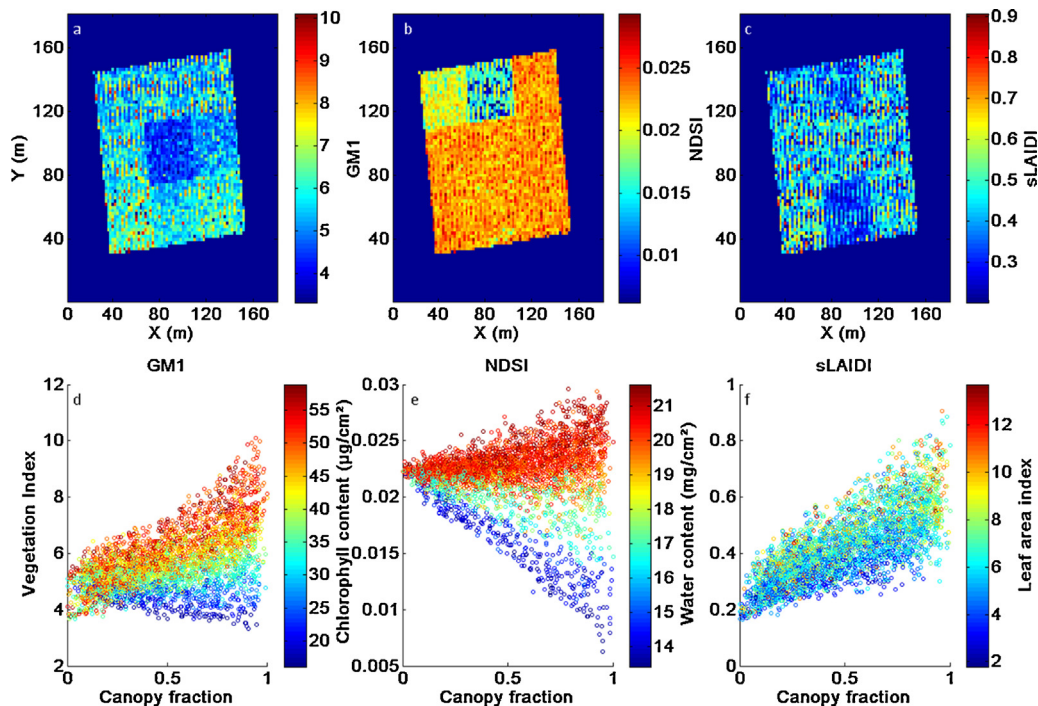


Fig. 6. Variable weed background synthetic images and scatter plots before correction of the GM1 index (a and d), the NDSI (b and e) and the sLAI (c and f). All points were labeled for chlorophyll content ( $\mu\text{g}/\text{cm}^2$ ), water content ( $\text{mg}/\text{cm}^2$ ) and leaf area index.

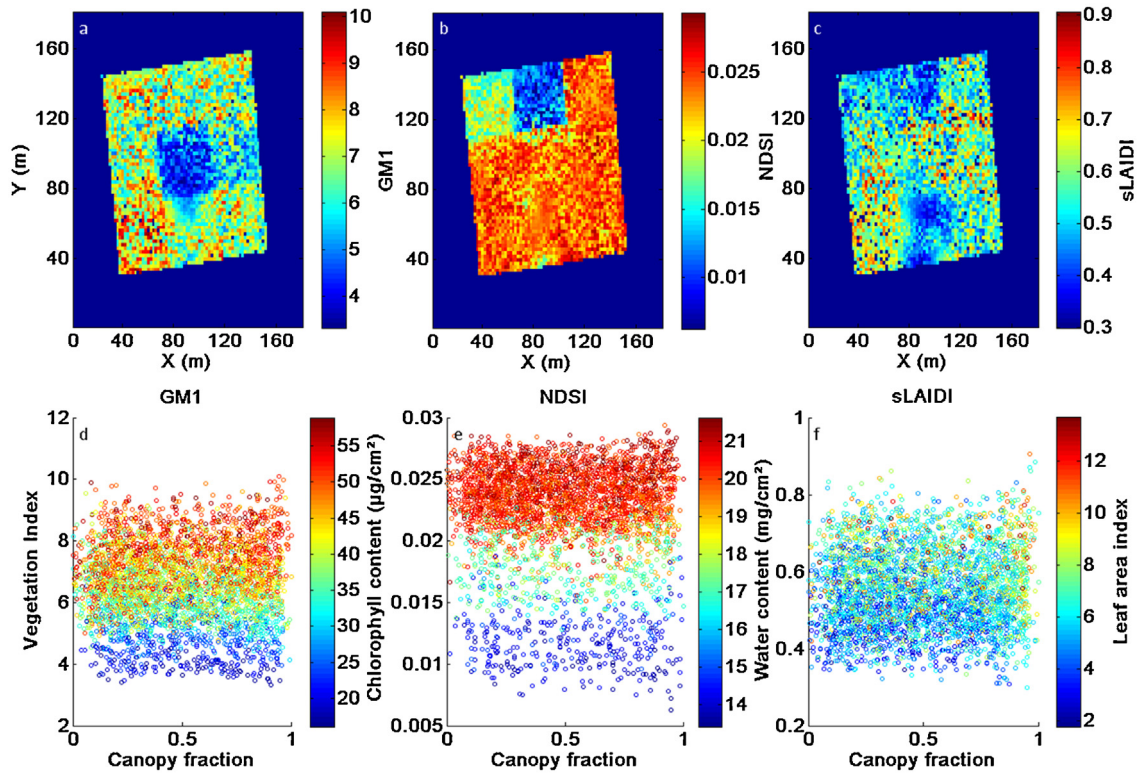


Fig. 7. Variable weed background synthetic images and scatter plots after correction of the GM1 index (a and d), the NDSI (b and e) and the sLAIDI (c and f). All points were labeled for chlorophyll content ( $\mu\text{g}/\text{cm}^2$ ), water content ( $\text{mg}/\text{cm}^2$ ) and leaf area index.

was Spindle bush system and others were V-system; Sansavini and Musacchi, 1994) and age differences (i.e. younger northern block). These differences were manifested as different canopy and background cover fractions, resulting in a flawed comparison between the different blocks. Furthermore, the alternation between pure and mixed pixels resulted in a striped effect in the satellite image (Fig. 8b), similar to the synthetic images in previous sections.

The correction removed the unwanted striping and reduced most of the background interference (Fig. 8c). In addition, some potentially stressed regions in the central block were highlighted, with higher ReNDVI values significant of higher stress levels (Van Beek et al., 2013). The highlighted region in the middle of the central block was the result of geographic differences, i.e. higher elevation and soil profile (Fig. 8a), which drained more easily and caused stressed canopies. As the image was taken during a period without significant differences between management treatments, no significant differences were expected. However, based on the uncorrected image, faulty management decisions could have been taken, which could have resulted in increased management costs or even decreased production.

## 5. Discussion

In general, larger differences between background and canopies caused larger influences on the vegetation indices, as was the case for S1 (Fig. 3). However, even for similar backgrounds and targets (e.g. S2 and S3), a correction was required. For example, in the variable weed background scenario, canopies with a high chlorophyll content (over  $50 \mu\text{g}/\text{cm}^2$ ) were represented by GM1 index values between 8 and 10 for pure canopy pixels, while the range of GM1 index values for mixed pixels (50% canopy cover fraction) decreased to between 5 and 7. Without considering this error, the mixed canopy pixels would correspond to a chlorophyll content of  $30 \mu\text{g}/\text{cm}^2$ . Compared to field studies in citrus orchards, this

drop would signify the difference between mature healthy leaves and sunburnt leaves or the difference between summer and winter leaves (Stuckens et al., 2011).

Through the generic vegetation index correction (Section 3.4), the background influence was reduced irrespective of background type (Figs. 4 and 7). Although less visible for S3 (Fig. 7), the correction removed canopy fraction dependency from the vegetation index values and hereby also removed differences within one management block. Compared to other correction methods, the vegetation index correction was shown equally or better equipped to reduce background effects. The soil-adjusted vegetation indices (TCARI/OSAVI and MCARI/OSAVI) were shown ineffective to correct the background effects in S1 (Section 4.1.2), as a result of the relatively low planting density and spatial resolution. In the past, the TCARI/OSAVI ratios were successfully applied to imagery with a higher spatial resolution in combination with tree border delineation (Zarco-Tejada et al., 2004) and larger planting densities (Haboudane et al., 2002). For these conditions, relatively constant canopy fractions were present (Haboudane et al., 2002). For imagery with highly variable canopy cover fractions, both TCARI/OSAVI and MCARI/OSAVI index ratios were not sufficient. Even though the signal unmixing method (ALS; Section 3.3.2) was shown to remove most of the soil background influence in S1 (Section 4.1.2), the performance of ALS was severely hampered by the spectral similarity of canopies and weeds in S2 (Section 4.2.1) and thus does not provide a generic solution to the mixture problem.

One of the requirements for the vegetation index correction was the knowledge of canopy cover fractions for the entire orchard. In this study, the cover fractions were either available (synthetic imagery, Sections 4.1 and 4.2) or determined based on a high resolution pan-sharpened image (real imagery, Section 4.3). However, the cover fraction might not be available in an operational setting. Several techniques could be used to estimate the cover fractions based



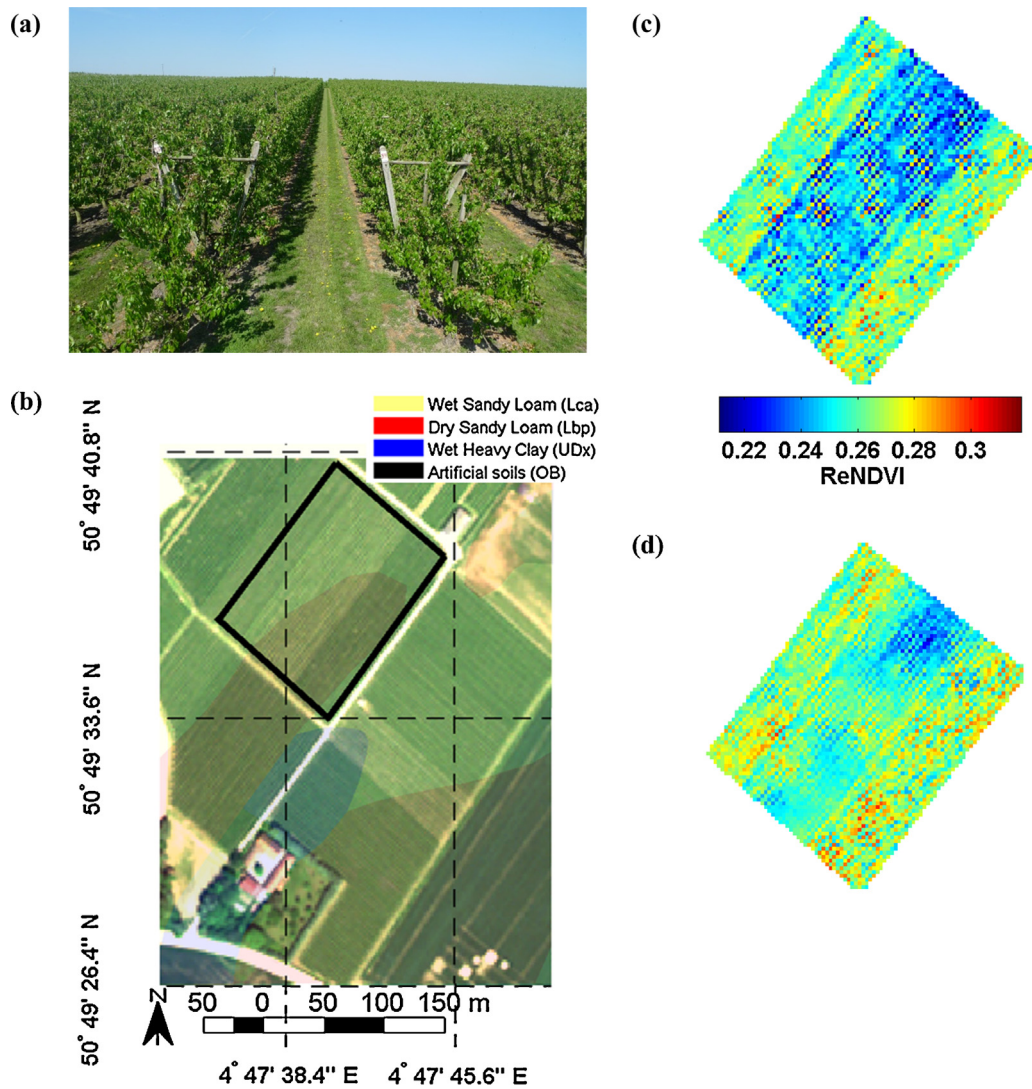


**Fig. 8.** Side view of V-shaped training system used in the study area (a); WorldView-2 satellite image (RGB) taken over an irrigated pear orchard in Bierbeek, Belgium (b), together with the uncorrected (c) and corrected vegetation index image (d) of a subsection of the orchard (highlighted in (b)).

on spectral differences (e.g. Multiple End member Spectral Mixture Analysis or MESMA; Roberts et al., 1998), which could estimate canopy cover fractions despite variable conditions and spectral similarity (Somers et al., 2011; Tits et al., 2013b). On the other hand, as orchards are built up as repetitive systems, orchard structure and canopy fractions could also be determined with simple metrics (i.e. planting distance, row distance and row orientation). Moreover, also image-based measurements could be used for large scale operations, such as the automatic detection and segmentation of orchards (Aksoy et al., 2012).

A persistent problem for this type of high resolution imagery is accounting for the within-canopy variability, causing low correlations with canopy derived variables (i.e. LAI;  $R^2 < 0.2$ ). For lower spatial resolution imagery the within-canopy variability is not a problem (e.g. Tits et al., 2013b), as the entire canopy is contained into one pixel. However, the gaps in the canopy caused spectral differences, not reflected in the biophysical variable. As the variation for the vegetation index was not related to canopy cover fraction, the correction method could not mitigate the effect (Section 3.4). Other studies in high resolution remote sensing avoided this problem by segmenting or classifying the canopies into sunlit and shaded areas, therefore avoiding these issues (Stagakis et al., 2012; Zarco-Tejada et al., 2004). However,

further research might be required to solve the within-canopy variability problem, as problems were enlarged for hedgerow systems.

Through the use of this generic solution to the mixture problem, the background effect could be removed from the satellite imagery over orchards. However, one of the assumptions made in this study was the presence of the full range of canopy fraction distributions. The presence of an off-nadir viewing angle, as is common for high resolution satellite imagery, would result in decreased background presence and negating the mixture problem (Stuckens et al., 2010). However, in hedgerow cropping systems larger viewing could also obstruct the relationship between biophysical variables and spectral measurements as the predominantly shaded side was imaged (Van Beek et al., 2013). Through the proposed correction, background effects within an orchard could be corrected for without prior knowledge or field measurements of the studied area. From these corrected vegetation indices, spatial differences within each management block and between management blocks could be highlighted and the production system could be optimized through already developed vegetation indices related to chlorophyll content (Zarco-Tejada et al., 2004) or water status (Van Beek et al., 2013). Moreover, future satellite missions such as WorldView-3 could offer more possibilities toward the application in orchards,

through the inclusion of Shortwave Infrared bands (1200–2500 nm) at high spatial resolutions (van der Meer et al., 2014), although the proposed correction would still be required. In addition, through the removal of spatial differences related to canopy cover fractions, age or growing systems, faulty management decisions leading to increased production costs or production losses could be avoided. Moreover, because the proposed correction standardized the vegetation indices images, useful comparison between images should be possible. Therefore, agricultural systems could be monitored throughout the growing season and a decision support system based on remote sensing information should be achievable. On the other hand, high spatial resolution satellite time series will always present variable viewing angles, which could influence spectral measurements (Stuckens et al., 2011) and index values. As a result, prior to the application of remote sensing for precision agriculture in horticulture, further research is required focusing on the influence of off-nadir view angles within time series.

## 6. Conclusions

Satellite remote sensing could be useful for precision agriculture applications in horticulture. However, high spatial resolutions are causing mixtures of canopies and background (i.e. soil, grass and shadow), hampering the estimation of these biophysical variables. In this study, this mixture problem in orchards was addressed. Through synthetic images, the problem was demonstrated and validated through the estimation of biophysical variables (i.e. chlorophyll, water content and leaf area index). Furthermore, a method to remove the influence of the canopy discontinuity on the vegetation indices was provided and its use demonstrated on synthetic images with different background and on a WorldView-2 satellite image.

For uniform soil and weed backgrounds, the vegetation indices were highly dependent on the underlying canopy fraction. Through a simple correction method, mixture problems were avoided and only relevant information was maintained. Moreover, for variable background scenario's a moving window approach was required to obtain similar results in a virtual setting and for real satellite imagery.

In a real-life setting, the study showed that prior to correction; only pure canopy pixels were useful toward the estimation of biophysical variables. After the correction, spatial differences within each management block and between management blocks would be related to changes in biophysical variables and not to differences in canopy cover fraction, age or growing system. As a result, the correction was found a useful tool for precision agriculture in orchards and could circumvent faulty management decisions; lower management costs and avoid production losses.

## Acknowledgments

This work was supported by the Agency for Innovation by Science and Technology in Flanders (IWT-Vlaanderen). The research was funded through a project (IWT 090924) in cooperation with the Soil Service of Belgium (BDB) and Proefcentrum Fruitteelt (PC Fruit). In addition, the authors would like to thank Jan Vandervelpen for allowing research in the orchard and making this research possible. Finally, the authors would like to acknowledge Dr. Jan Stuckens for his research regarding the virtual orchard and making this work possible.

## References

Acevedo-Opazo, C., Tisseyre, B., Guillaume, S., Ojeda, H., 2008. The potential of high spatial resolution information to define within-vineyard zones related to vine water status. *Precis. Agric.* 9 (5), 285–302.

- Adler-Golden, S.M., Berk, A., Bernstein, L.S., Richtsmeier, S., Acharya, P.K., Matthew, M.W., Anderson, G.P., et al., 1998. FLAASH, a MODTRAN4 atmospheric correction package for hyperspectral data retrievals and simulations. In: Green, R.O. (Ed.), *Summaries of the Seventh JPL Airborne Earth Science Workshop*, January 12–16, 1998, p. 442.
- Aksay, S., Yalniz, I.Z., Tasdemir, K., 2012. Automatic detection and segmentation of orchards using very high resolution imagery. *IEEE Trans. Geosci. Remote Sens.* 50 (8), 3117–3131.
- Delalieux, S., Somers, B., Hereijgers, S., Verstraeten, W., Keulemans, W., Coppin, P., 2008. A near-infrared narrow-waveband ratio to determine leaf area index in orchards. *Remote Sens. Environ.* 112 (10), 3762–3772.
- Dorigo, W.A., Zurita-Milla, R., de Wit, A.J.W., Brazile, J., Singh, R., Schaepman, M.E., 2007. A review on reflective remote sensing and data assimilation techniques for enhanced agroecosystem modeling. *Int. J. Appl. Earth Observ. Geoinf.* 9 (2), 165–193.
- FAO, 1988. *Soils Map of the World: Revised Legend*. Food and Agriculture Organization of the United Nations, Rome.
- Gitelson, A.A., Merzlyak, M.N., 1996. Signature analysis of leaf reflectance spectra: algorithm development for remote sensing of chlorophyll. *J. Plant Physiol.* 148 (3–4), 494–500.
- Govender, M., Dye, P.J., Weiersbye, I.M., Witkowski, E.T.F., Ahmed, F., 2009. Review of commonly used remote sensing and ground-based technologies to measure plant water stress. *Water SA* 35 (5), 741–752.
- Haboudane, D., Miller, J.R., Tremblay, N., Zarco-Tejada, P.J., Dextraze, L., 2002. Integrated narrow-band vegetation indices for prediction of crop chlorophyll content for application to precision agriculture. *Remote Sens. Environ.* 81 (2–3), 416–426.
- Hamada, Y., Stow, D.A., Roberts, D.A., 2011. Estimating life-form cover fractions in California sage scrub communities using multispectral remote sensing. *Remote Sens. Environ.* 115 (12), 3056–3068.
- Hosgood, B., Jacquemoud, S., Andreoli, G., Verdebout, J., Pedrini, A., Schmuck, G., 1994. Leaf Optical Properties EXperiment 93 (LOPEX93). Report EUR 16095 EN. European Commission – Joint Research Centre, Ispra.
- Huete, A.R., 1988. A soil-adjusted vegetation index (SAVI). *Remote Sens. Environ.* 25, 295–309.
- Jacquemoud, S., Baret, F., 1990. Prospect: a model of leaf optical properties spectra. *Remote Sens. Environ.* 34, 75–91.
- Laben, C.A., Brower, B.V., 2000. Process for enhancing the spatial resolution of multispectral imagery using pan-sharpening. United States Eastman Kodak Company. US Patent 6011875.
- Laurikkala, J., Juhola, M., Kentala, E., 2000. Informal identification of outliers in medical data. In: Fifth International Workshop on Intelligent Data Analysis in Medicine and Pharmacology IDAMAP-2000. Organized as a workshop of the 14th European Conference on Artificial Intelligence ECAI-2000, Berlin, 22 August.
- Marchisio, G., Pacifici, F., Padwick, C., 2010. On the relative predictive value of the new spectral bands in the WorldView-2 sensor. In: IGARSS, pp. 2723–2726.
- Moran, S., Fitzgerald, G., Rango, A., Walthall, C., Barnes, E., Bausch, W., Clarke, T., et al., 2003. Sensor development and radiometric correction for agricultural applications. *Photogramm. Eng. Remote Sens.* 69 (6), 705–718.
- Perry, E.M., Dezzani, R.J., Seavert, C.F., Pierce, F.J., 2009. Spatial variation in tree characteristics and yield in a pear orchard. *Precis. Agric.* 11 (1), 42–60.
- Pharr, M., Humphreys, G., 2004. *Physically Based Rendering, From Theory to Implementation*. Morgan Kaufmann, San Francisco, CA, pp. 1019.
- Pinter, P.J., Hatfield, J.L., Schepers, J.S., Barnes, E.M., Moran, M.S., Daughtry, C.S.T., Upchurch, D.R., 2003. Remote sensing for crop management. *Photogramm. Eng. Remote Sens.* 69 (6), 647–664.
- Roberts, D.A., Gardner, M., Church, R., Ustin, S., Scheer, G., 1998. Mapping chaparral in the Santa Monica mountains using multiple endmember spectral mixture models. *Remote Sens. Environ.* 65, 267–279.
- Rondeaux, G., Steven, M., Baret, F., 1996. Optimization of soil-adjusted vegetation indices. *Remote Sens. Environ.* 107, 95–107.
- Sansavini, S., Musacchi, S., 1994. Canopy architecture, training and pruning in the modern European pear orchards: an overview. *Acta Hort.* (ISHS) 367, 152–172.
- Somers, B., Asner, G.P., Tits, L., Coppin, P., 2011. Endmember variability in spectral mixture analysis: a review. *Remote Sens. Environ.* 115 (7), 1603–1616.
- Somers, B., Delalieux, S., Verstraeten, W.W., Coppin, P., 2009. A conceptual framework for the simultaneous extraction of sub-pixel spatial extent and spectral characteristics of crops. *Photogramm. Eng. Remote Sens.* 75 (1), 57–68.
- Somers, B., Gysels, V., Verstraeten, W.W., Delalieux, S., Coppin, P., 2010. Modelling moisture-induced soil reflectance changes in cultivated sandy soils: a case study in citrus orchards. *Eur. J. Soil Sci.* 61 (6), 1091–1105.
- Stagakis, S., González-Dugo, V., Cid, P., Guillén-Climent, M.L., Zarco-Tejada, P.J., 2012. Monitoring water stress and fruit quality in an orange orchard under regulated deficit irrigation using narrow-band structural and physiological remote sensing indices. *ISPRS J. Photogramm. Remote Sens.* 71, 47–61.
- Stuckens, J., Dzikiti, S., Verstraeten, W.W., Verreynne, S., Swennen, R., Coppin, P., 2011. Physiological interpretation of a hyperspectral time series in a citrus orchard. *Agric. For. Meteorol.* 151 (7), 1002–1015.
- Stuckens, J., Somers, B., Albrigo, G.L., Dzikiti, S., Verstraeten, W.W., 2010. Off-nadir viewing for reducing spectral mixture issues in citrus orchards. *Photogramm. Eng. Remote Sens.* 76 (11), 1261–1274.
- Stuckens, J., Somers, B., Delalieux, S., Verstraeten, W.W., Coppin, P., 2009. The impact of common assumptions on canopy radiative transfer simulations: a

- case study in Citrus orchards. *J. Quant. Spectrosc. Radiat. Transfer* 110 (1-2), 1–21.
- Tauler, R., Kowalski, B., Fleming, S., 1993. Multivariate curve resolution applied to spectral data from multiple runs of an industrial process. *Anal. Chem.* 65 (15), 2040–2047.
- Tits, L., Somers, B., Saeys, W., Coppin, P., 2013a. Alternating least-squares unmixing for the extraction of sub-pixel information from agricultural areas. *Proc. SPIE* 8887, 888706–888710.
- Tits, L., Somers, B., Stuckens, J., Farifteh, J., Coppin, P., 2013b. Integration of in situ measured soil status and remotely sensed hyperspectral data to improve plant production system monitoring: concept, perspectives and limitations. *Remote Sens. Environ.* 128, 197–211.
- Tou, J.T., Gonzalez, R.C., 1974. *Pattern Recognition Principles*. Addison-Wesley Publishing Company, Reading, MA, pp. 377.
- Updike, T., Comp, C., 2010. *Radiometric Use of WorldView-2 Imagery*. Technical Note., pp. 16.
- Van Beek, J., Tits, L., Somers, B., Coppin, P., 2013. Stem water potential monitoring in pear orchards through WorldView-2 multispectral imagery. *Remote Sens.* 5 (12), 6647–6666.
- Weber, J., Penn, J., 1995. Creation and rendering of realistic trees. In: *Proceedings of the 22nd Annual Conference on Computer Graphics and Interactive Techniques*, pp. 119–128.
- Zarco-Tejada, P., Miller, J., Morales, A., Berjón, A., Agüera, J., 2004. Hyperspectral indices and model simulation for chlorophyll estimation in open-canopy tree crops. *Remote Sens. Environ.* 90 (4), 463–476.
- van der Meer, F.D., van der Werff, H.M.A., van Ruitenbeek, F.J.A., 2014. Potential of ESA's Sentinel-2 for geological applications. *Remote Sens. Environ.* 148, 124–133.